iScience

CellPress
OPEN ACCESS

Article

Single-cell transcriptomics reveals subset-specific metabolic profiles underpinning the bronchial epithelial response to flagellin

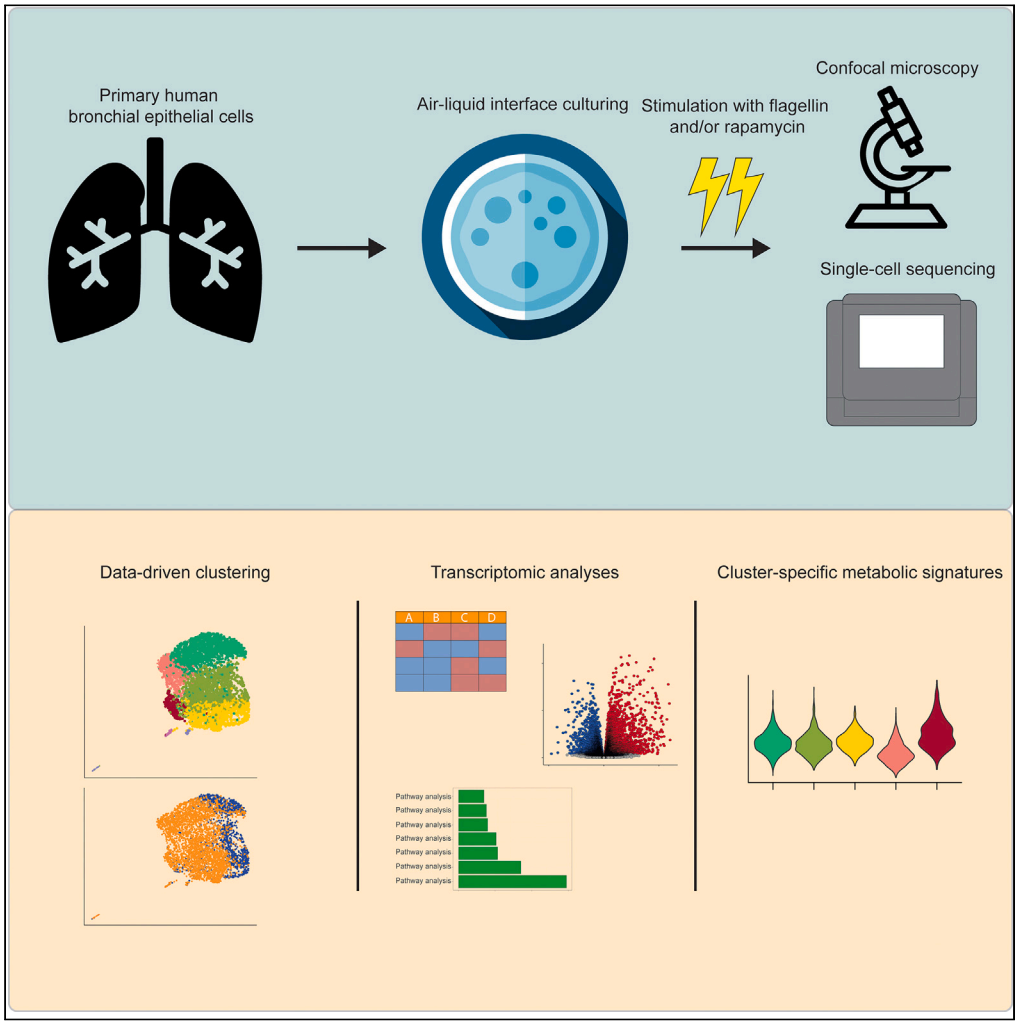

Ivan Ramirez-Moral, Alex R. Schuurman, Christine C.A. van Linge, ..., Menno D. de Jong, Felipe A. Vieira Braga, Tom van der Poll

t.vanderpoll@amsterdamumc.nl

Highlights

Single-cell RNA sequencing identified seven cell clusters in human airways

Flagellin selectively increased inflammatory basal and secretory cells

Flagellin enhanced aerobic glycolysis in inflammatory secretory cells

mTOR inhibition prevented glycolysis and reduced inflammation in this cell subset

Ramirez-Moral et al., iScience 27, 110662
September 20, 2024
https://doi.org/10.1016/j.isci.2024.110662

iScience

CellPress
OPEN ACCESS

Article

Single-cell transcriptomics reveals subset-specific metabolic profiles underpinning the bronchial epithelial response to flagellin

Ivan Ramirez-Moral,[1,5] Alex R. Schuurman,[1,5] Christine C.A. van Linge,[1] Joe M. Butler,[1] Xiao Yu,[2] Karen de Haan,[2] Sarah van Leeuwen,[2] Alex F. de Vos,[1] Menno D. de Jong,[2] Felipe A. Vieira Braga,[3,6] and Tom van der Poll[1,4,6,7,*]

SUMMARY

Airway epithelial cells represent the first line of defense against respiratory pathogens. Flagellin drives the motility of many mucosal pathogens and has been suggested as an immune enhancing adjunctive therapeutic in infections of the airways. This study leveraged single-cell RNA sequencing to determine cell-specific effects of flagellin in primary human bronchial epithelial cells growing in air-liquid interface. Seven cell clusters were identified, including ciliated cells, ionocytes, and several states of basal and secretory cells, of which only inflammatory basal cells and inflammatory secretory cells demonstrated a proportional increase in response to flagellin. Inflammatory secretory cells showed evidence of metabolic reprogramming toward aerobic glycolysis, while in inflammatory basal cells transcriptome profiles indicated enhanced oxidative phosphorylation. Inhibition of mTOR prevented the shift to glycolysis and reduced inflammatory gene transcription specifically in inflammatory secretory cells. These data demonstrate the functional heterogeneity of the human airway epithelium upon exposure to flagellin.

INTRODUCTION

The human airways represent a major interface between the environment, which is teeming with potentially pathogenic microbes, and the inner body. The epithelium that lines the airways is responsible for maintaining immune homeostasis in the lung, while also offering protection to microorganisms and pollutants that we inhale.[1,2] Over the last decade, the field of immunometabolism has solidified the concept that regulation of the different energy pathways within cells is key in maintaining and shaping the immune response to infection.[3–6] We recently engaged in studies on the role of metabolism in the immune function of the airway's epithelium,[7,8] and showed that activation of primary human bronchial epithelial (HBE) cells in response to flagellin – a bacterial component that is typically present on the surface of mucosal pathogens[9,10] – is regulated by mammalian target of rapamycin (mTOR)-driven glycolysis.[7] Purified and recombinant flagellin can activate Toll-like receptor (TLR)5, a pattern recognition receptor that is strongly expressed at the surface of epithelial cells, triggering signaling events that eventually result in activation of nuclear factor-κB and production of cytokines, chemokines, and defensins. Local activation of TLR5 in the airways by topically administered flagellin improved innate immune defense against lower respiratory tract infection induced by several bacterial species.[9,11] Thus, knowledge of the mechanisms by which flagellin activates the respiratory epithelium is not only of relevance for understanding local inflammatory responses induced by flagellated pathogens, but also considering the potential application of flagellin as an immune enhancing therapy during infection of the lungs.[9,11–16]

The human airway epithelium consists of a heterogeneous community of different cell types, each with unique molecular characteristics.[2] Traditionally, four major cell types have been recognized in the airway epithelial layer, i.e., secretory club cells, goblet cells, ciliated cells, and basal cells.[2] More recently, single-cell RNA sequencing (scRNA-seq) identified additional subsets of airway epithelial cells, indicating that the cellular landscape of the airway epithelium is more heterogeneous than previously thought.[2,17–19] While it is likely that these different cell types, which fulfill distinct functions during the immune response against infection, are driven by specific metabolic programs, this remains to be investigated.

[1]Center of Experimental and Molecular Medicine, Amsterdam Infection & Immunity Institute, Amsterdam UMC, University of Amsterdam, Meibergdreef 9, 1105 AZ Amsterdam, the Netherlands
[2]Department of Medical Microbiology, Amsterdam UMC, University of Amsterdam, Meibergdreef 9, 1105 AZ Amsterdam, the Netherlands
[3]Laboratory for Experimental Oncology and Radiobiology, Center of Experimental and Molecular Medicine, Cancer Center Amsterdam and Amsterdam Gastroenterology and Metabolism, Amsterdam UMC, University of Amsterdam, Meibergdreef 9, 1105 AZ Amsterdam, the Netherlands
[4]Division of Infectious Diseases, Amsterdam UMC, University of Amsterdam, Meibergdreef 9, 1105 AZ Amsterdam, the Netherlands
[5]These authors contributed equally
[6]These authors contributed equally
[7]Lead contact
*Correspondence: t.vanderpoll@amsterdamumc.nl
https://doi.org/10.1016/j.isci.2024.110662

Previously, we showed that flagellin activates HBE cells at least in part by stimulation the mTOR pathway.[7] Indeed, inhibition of mTOR by rapamycin reduced the expression of genes encoding a variety of chemokines and antimicrobial peptides in HBE cells exposed to flagellin.[7] Notably, these analyses were done on lysates of bulk HBE cells, thereby precluding studies on the role of specific cell subsets within these cultures. In the current study, we sought to determine the role of distinct cell types in HBE cell cultures in mTOR-driven immune responses triggered by flagellin. For this we leveraged scRNA-seq, which enables us to individually analyze thousands of cells from a complex system, such as the airway epithelium, and to identify cell subsets with unique transcriptomic profiles. We hypothesized that secretory (club and goblet) cells are the main drivers of flagellin-induced activation of the respiratory epithelium considering their earlier described capacity to produce inflammatory mediators and antimicrobial peptides.[2]

RESULTS

HBE cells were harvested from healthy tracheobronchial tissue obtained during lobectomy surgery and differentiated in the air-liquid interface as previously described.[7] This approach yielded fully differentiated HBE cells constituting three cell types – basal, secretory, and ciliated cells – in a basal-to-apical orientation as shown by confocal microscopy (Figure 1A). After quality control, the transcriptome of 6577 single HBE cells across three experimental conditions was analyzed: unstimulated (vehicle; PBS), stimulated with flagellin, or flagellin-stimulated in the presence of rapamycin.

Increased proportions of inflammatory basal and secretory cells upon stimulation with flagellin

The epithelial response to flagellin was initially explored in comparison to unstimulated cells. Based on the transcriptome of all individual cells from these two conditions, seven cell clusters were identified, as visualized by Uniform Manifold Approximation and Projection (UMAP) dimensionality reduction (Figure 1B). Clusters were annotated based on canonical marker genes among the top differentially expressed genes (DEGs) between clusters (see Table S1 for an overview[2,20]), which revealed three clusters of basal cells and two clusters of secretory (goblet) cells, as well as ionocytes and ciliated cells (Figure 1B). Two of the three basal cell states reflected different differentiation stages: relatively high KRT5 and KRT15 expression suggests that basal 1 cells were more stem-like while basal 2 cells were more mature. The third basal subset was labeled as inflammatory based on high expression of S100 members S100A8 and S100A9 and other inflammatory mediators such as CCL20. Secretory cells were characterized by high expression of the canonical markers[2,20] SCGB1A1, MUC5B and SCGB3A1. An inflammatory secretory subset was identified based on high expression of the genes encoding for the inflammatory mediators CXCL8, CXCL16 and G-CSF, among others. In addition, consistent proportions of p63 and MUC5B^{+} cells after flagellin activation, with induced CXCL1 production in both subsets compared to control were confirmed by flow cytometry analysis (Figure S1). To assess the robustness of this secretory inflammatory cluster we isolated the data for all secretory cells and re-clustered the cells, which again revealed the distinct inflammatory cluster (Figure S2A). Ciliated cells were identified by high levels of the canonical marker genes PIFO and FOXJ1. Ionocytes were defined by high expression of FOXI1. The top 10 DEGs, not only including canonical genes, between the identified clusters are depicted in Figure 1C. Next, the effect of flagellin on the composition of the HBE cells was assessed (Figure 1D shows the UMAP colored per condition). Flagellin induced profound differences in the proportional composition of the identified cell clusters. Specifically, a lower proportion of basal 1 and secretory cells, and a higher proportion of basal inflammatory and secretory inflammatory cells were found in the flagellin condition (Figure 1E). No differences in the proportion of basal 2 cells, ciliated cells, or ionocytes after flagellin stimulation were observed. As the ciliated cell cluster and ionocyte cluster represented very few cells and showed no proportional change in the flagellin condition, further studies focused on the basal and secretory cell clusters.

The transcriptional landscape of inflammatory basal and secretory cells

As only the inflammatory subclusters of the basal and secretory cells were clearly more abundant in the flagellin condition, the transcriptional profiles of these inflammatory subclusters were investigated next. Upon comparison of the secretory inflammatory cells to the other secretory cells, genes coding for the prototypic epithelial-inflammatory mediators were up-regulated in the secretory inflammatory cells (CCL20, CXCL8, CSF3) as well as three keratin coding genes (KRT17, KRT15, KRT16) (Figure 2A). Interestingly, the gene coding for the enzyme responsible of the last reaction of the glycolysis pathway (LDHA) was highly expressed in the secretory inflammatory subset (Figure 2A). Basal inflammatory cells, relative to basal 1 cells, displayed a strong pro-inflammatory signature indicative of a heightened innate immune response, including upregulation of S100A8-9, several SERPIN genes, CXCL1, CXL8 and CCL20 (Figure 2B, see Figure S3 for basal inflammatory versus basal 2). Downregulated genes included two keratin coding genes (KRT5, KRT15), and two tropomyosin coding genes (TPM1, TPM2). Next, we sought to identify unique features between these two inflammatory subclusters. The Venn-Euler plot (Figure 2C) shows the result from the differential gene analysis directly comparing these subclusters, indicating the number of genes significantly upregulated in secretory inflammatory cells (255), upregulated in basal inflammatory cells (565) and non-significant genes (233). Pathway analysis was performed on the 255 upregulated genes in secretory inflammatory cells and the 565 upregulated genes in basal inflammatory cells (Figure 2C). Several of the upregulated pathways – such as hypoxia, the P53 pathway and TNF signaling via NFkB – were enriched in both cell types; androgen response genes were only upregulated in secretory inflammatory cells. These data suggest that cells in both clusters showed transcriptional signs of stress and inflammation. Interestingly however, only the secretory inflammatory cells had upregulated glycolysis and MTOR signaling pathways, while basal inflammatory cells showed upregulated transcripts involved in oxidative phosphorylation. This implies a subset-specific metabolic switch in response to flagellin. These data expand upon our previous work, indicating that the activation of mTOR-mediated

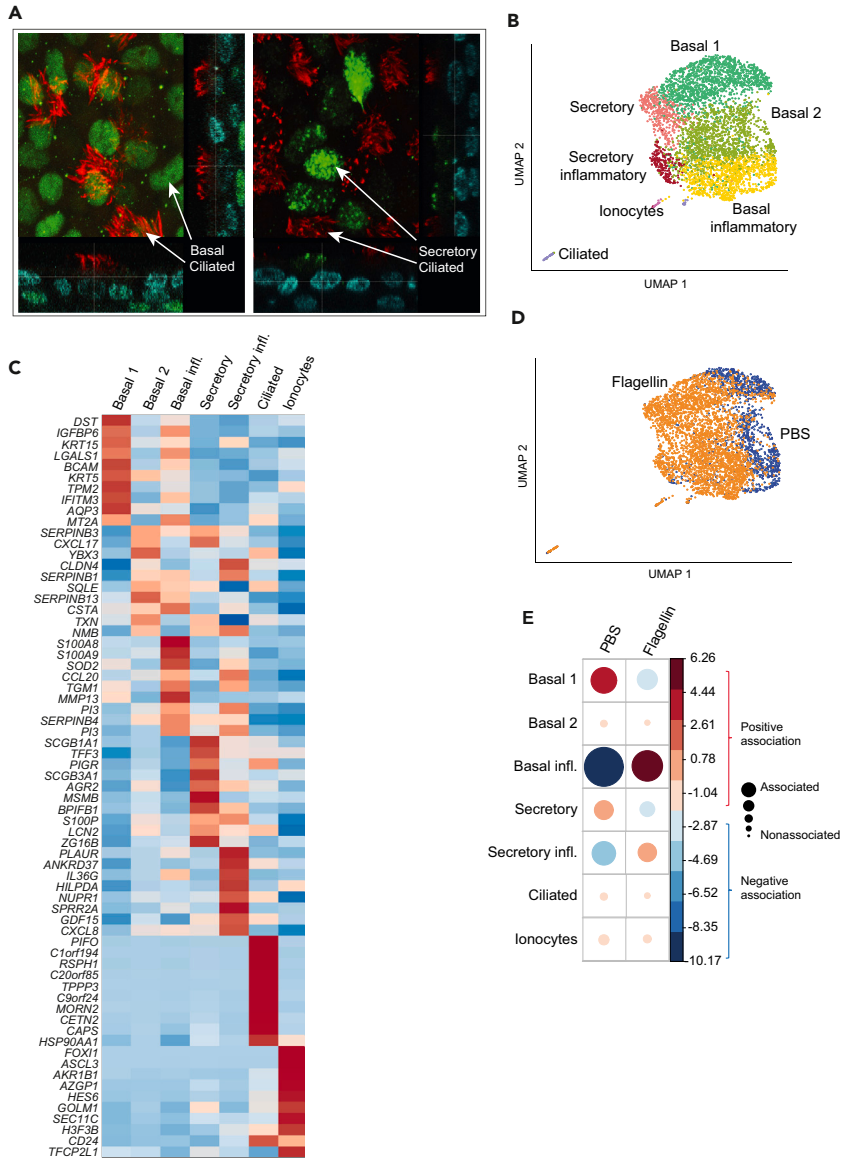

Figure 1. Primary human bronchial epithelial cell cultures show a proportional increase of basal inflammatory and secretory inflammatory cells upon stimulation with flagellin

(A) Confocal imaging of polarized HBE cells; in red β-tubulin$^+$ ciliated cells, blue nuclei (DAPI), green (left panel) p63$^+$ basal cells and green (right panel) MUC5B$^+$ secretory cells. Max. projection.

(B) UMAP of HBE cells, stimulated by either PBS or flagellin, where the color indicates the cluster as identified by single-cell transcriptomic analysis. Each dot represents one cell. Genes from the canonical markers used for cluster identification are listed in Table S1.

(C) Heatmap showing the expression of the top differentially expressed genes (DEGs) for each cluster, when compared to the rest of the clusters.

(D) Same as panel B, now colored by experimental condition.

(E) Correlation plot depicting cluster enrichment between the PBS and flagellin condition. Dot size is proportional to the Pearson's residual of the chi-squared test (reflecting the difference between the observed and expected proportion), while the color represents the degree of association from Pearson's chi-squared residuals (red is a positive association, blue is a negative association).

glycolysis in bulk HBE cells stimulated by flagellin[7] that we previously observed, could be driven by secretory inflammatory cells specifically. To further investigate this, the metabolic programming of the identified clusters was analyzed, and the effect of flagellin thereon.

Secretory inflammatory cells have a distinct metabolic profile of enhanced glycolysis and mTOR-signaling

The metabolic signature scores for amino acid metabolism, glycolysis, mTOR signaling, lipid metabolism and the tricarboxylic acid (TCA) cycle – derived from the hallmark gene sets in the Molecular Signatures Database[21] – between all basal and secretory clusters was compared. In

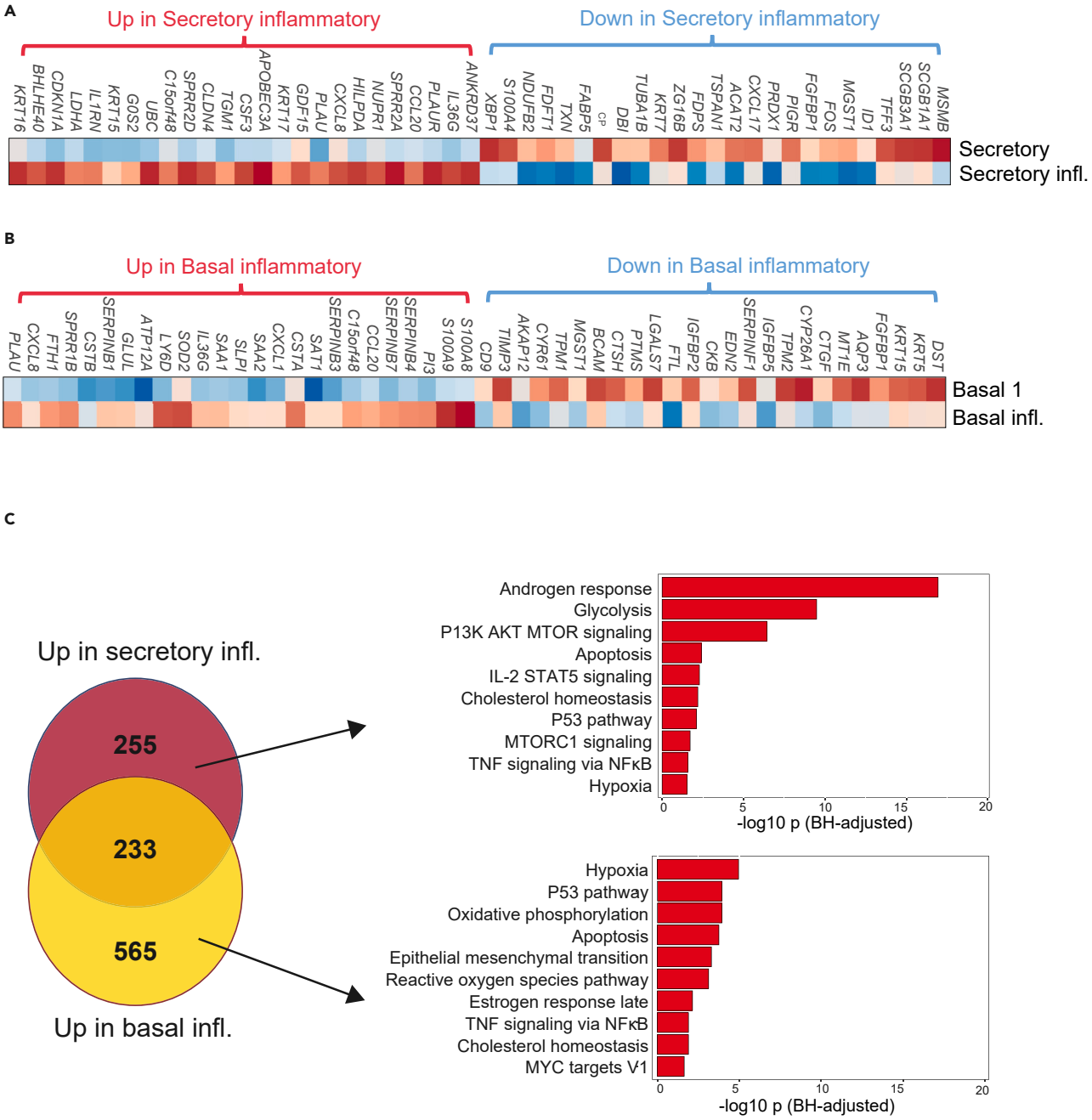

Figure 2. The transcriptional landscape of inflammatory basal and secretory cells

(A) Heatmap showing the expression of the top 25 increased and top 25 decreased DEGs derived from comparing the secretory and secretory inflammatory cells (log fold change >0.25, adjusted $p < 0.05$).

(B) Same as in panel A, but here the comparison is made between basal 1 and basal inflammatory cells.

(C) Venn-Euler plot depicting the result of differential gene expression analysis between secretory inflammatory and basal inflammatory cells. Molecular Signatures Database (MSigDB) pathway analysis was performed on the DEGs upregulated in secretory inflammatory cells (upper pathways), and on the DEGs upregulated in basal inflammatory cells (lower pathways). The X axis shows the Benjamini-Hochberg adjusted −log10 *p*-value from the enrichment score analysis.

line with the analysis in Figure 2C, glycolysis and mTOR signaling were clearly upregulated in secretory inflammatory cells when compared to the other subsets, including the other secretory cells (Figure 3A). The other metabolic pathways showed no major differences between subsets, although genes encoding for enzymes of the TCA cycle were relatively lowly expressed in secretory inflammatory cells and highly expressed in the other secretory subset, possibly indicating a metabolic shift from the TCA cycle to glycolysis, triggered by flagellin (Figure S4).

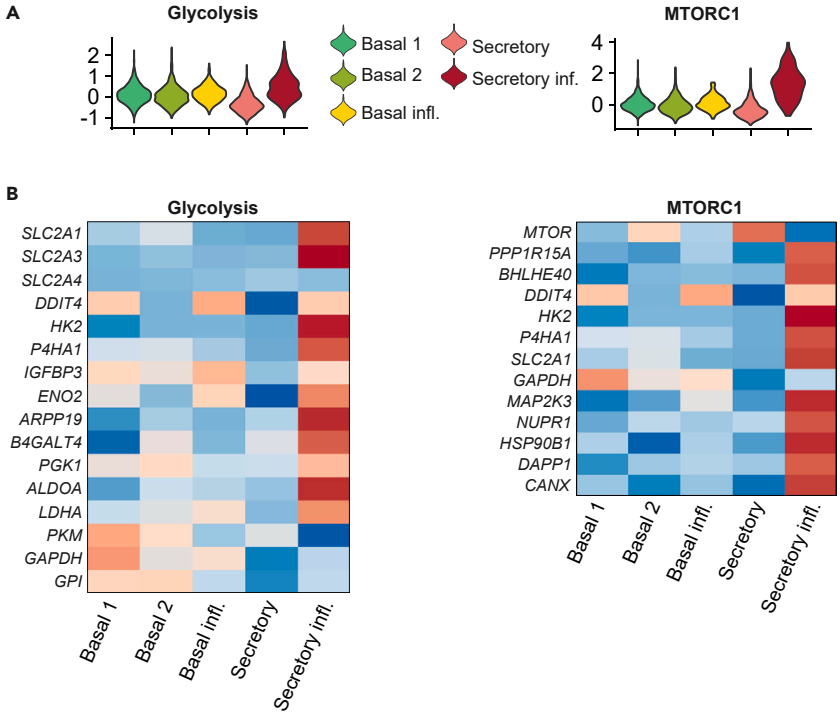

Figure 3. Secretory inflammatory cells have a distinct transcriptional profile of enhanced glycolysis and mTOR-signaling

(A) Violin plots of the metabolic gene signature scores for glycolysis and the mTOR signaling pathway between the cell clusters. Other metabolic signature scores are depicted in Figure S3.

(B) Heatmaps depicting the average scaled expression of genes related to glycolysis and the mTOR signaling pathway, split between the cell clusters.

Heatmaps of key genes in glycolysis and mTOR-signaling corroborated the gene signature scores, with clearly increased expression specifically in secretory inflammatory cells (Figure 3B).

Rapamycin induces a specific proportional decrease of secretory inflammatory cells

Our hypothesis was that mTOR-mediated glycolysis was key for the expansion of secretory inflammatory cells during stimulation with flagellin. To investigate whether mTOR-inhibition would affect this flagellin-induced change, HBE cells stimulated with flagellin in the presence or absence of rapamycin were compared. The same approach as in Figure 1 was applied, and seven cell clusters which we annotated based on the expression of canonical genes were recapitulated (see Table S1). Again, several states of basal cells and secretory cells were identified, as well as ionocytes and ciliated cells (Figure 4A). The secretory subclusters included two clusters that mainly differed based on the expression of genes from the SERPIN family (SERPINB3, SERPINB1, SERPINB4 and SERPINB7). Cells clustered as secretory 1 and secretory inflammatory expressed higher levels of SERPIN-related genes which are known for being involved in inflammatory and immune cellular responses.[22] Cells clustered as secretory 2 expressed the classical club cell markers[23] including genes related to mucous cell differentiation (TFF3 and AGR2) and growth factors related to host defense (LCN2 and BPIFB1). The secretory inflammatory cluster showed high expression of genes coding for inflammatory mediators (IL36G and CXCL8) (see Figure 4B for the top 10 DEGs of each cluster). The two identified basal states included the canonical markers described in Figure 1C, with increased expression of inflammatory genes in the basal inflammatory compartment (S100A8 and S100A9) (Figure 4B).

Next, the impact of rapamycin on the flagellin-stimulated cells was assessed (see Figure 4C for the UMAP colored per condition). Strikingly, a large proportional difference of the secretory inflammatory cluster was observed: secretory inflammatory cells were clearly less abundant in the presence of rapamycin (Figure 4D). The other clusters showed only subtle differences – with slightly higher proportions of basal inflammatory cells, secretory 2 cells and ionocytes in the rapamycin condition – in line with our hypothesis that rapamycin may specifically limit expansion of secretory inflammatory cells. To analyze whether this specific proportional decrease of secretory inflammatory cells was indeed related to impaired mTOR-signaling and glycolysis, the transcriptomic differences between the two conditions were assessed next.

Rapamycin induces a transcriptional profile of reduced glycolysis and inflammation, and decreases GLUT1 expression in secretory cells

Our group previously showed that rapamycin suppresses flagellin-induced glycolysis and mTOR signaling in bulk HBE cells.[7] Comparison of the metabolic and inflammatory gene signature scores induced by flagellin in the presence or absence of rapamycin within the

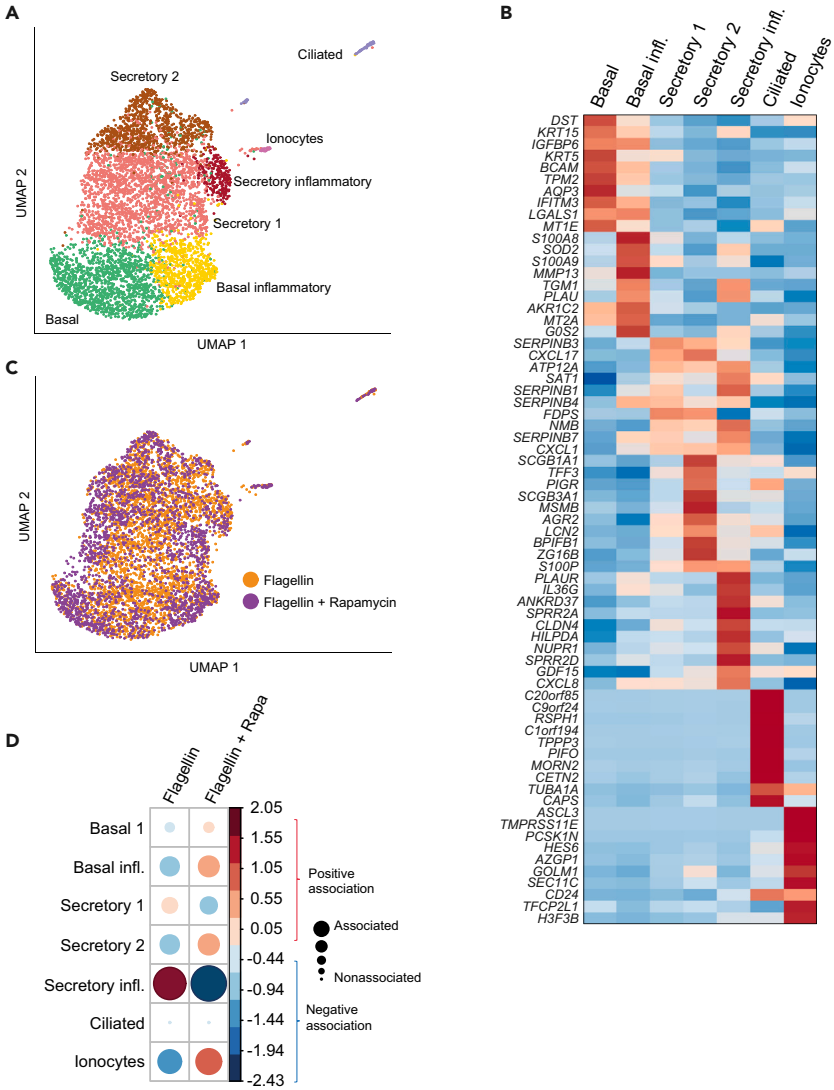

Figure 4. Rapamycin induces a specific proportional decrease of secretory inflammatory cells

(A) UMAP of HBE cells, stimulated by either flagellin or flagellin + rapamycin, color indicates the cluster as identified by single-cell transcriptomic analysis. Each dot represents one cell.

(B) Heatmap showing the expression of the top differentially expressed genes (DEGs) for each cluster. Genes from the canonical markers used for cluster identification are listed in Table S1.

(C) Same as panel A, now colored by experimental condition.

(D) Correlation plot depicting cluster enrichment between the flagellin and flagellin + rapamycin condition. Dot size is proportional to the Pearson's residual of the chi-squared test (reflecting the difference between the observed and expected proportion), while the color represents the degree of association from Pearson's chi-squared residuals (red is a positive association, blue is a negative association).

secretory cell metacluster confirmed that rapamycin downregulated mTOR-signaling, glycolysis and inflammatory genes (Figure 5A), whilst other metabolic pathways were slightly upregulated (Figure S5). Figure 5B depicts key genes in glycolysis – akin to Figure 3B – for the distinct secretory cell clusters and split between the conditions, showing that rapamycin induced downregulation of glycolytic genes in every subset of secretory cells. SLC2A1, the gene encoding GLUT1, was among the top downregulated genes by rapamycin in flagellin-stimulated bulk HBE cells (data not shown) and in the glycolysis gene pathway in secretory cells (Figure 5B). Confocal microscopy confirmed enhanced expression of GLUT1 in secretory cells in HBE cultures stimulated with flagellin; inhibition of the mTOR pathway by rapamycin limited the abundance of GLUT1 in these cells, losing the organization observed in the flagellin-only condition (Figure 5C). Importantly, rapamycin treatment only resulted in a proportional decrease of secretory inflammatory cells, and not the other secretory subsets, as shown in Figure 4D. Together these data indicate that flagellin induces a proportional increase of inflammatory cell subsets in the human airway epithelium, of which specifically secretory inflammatory cells rely on mTOR-signaling and glycolysis.

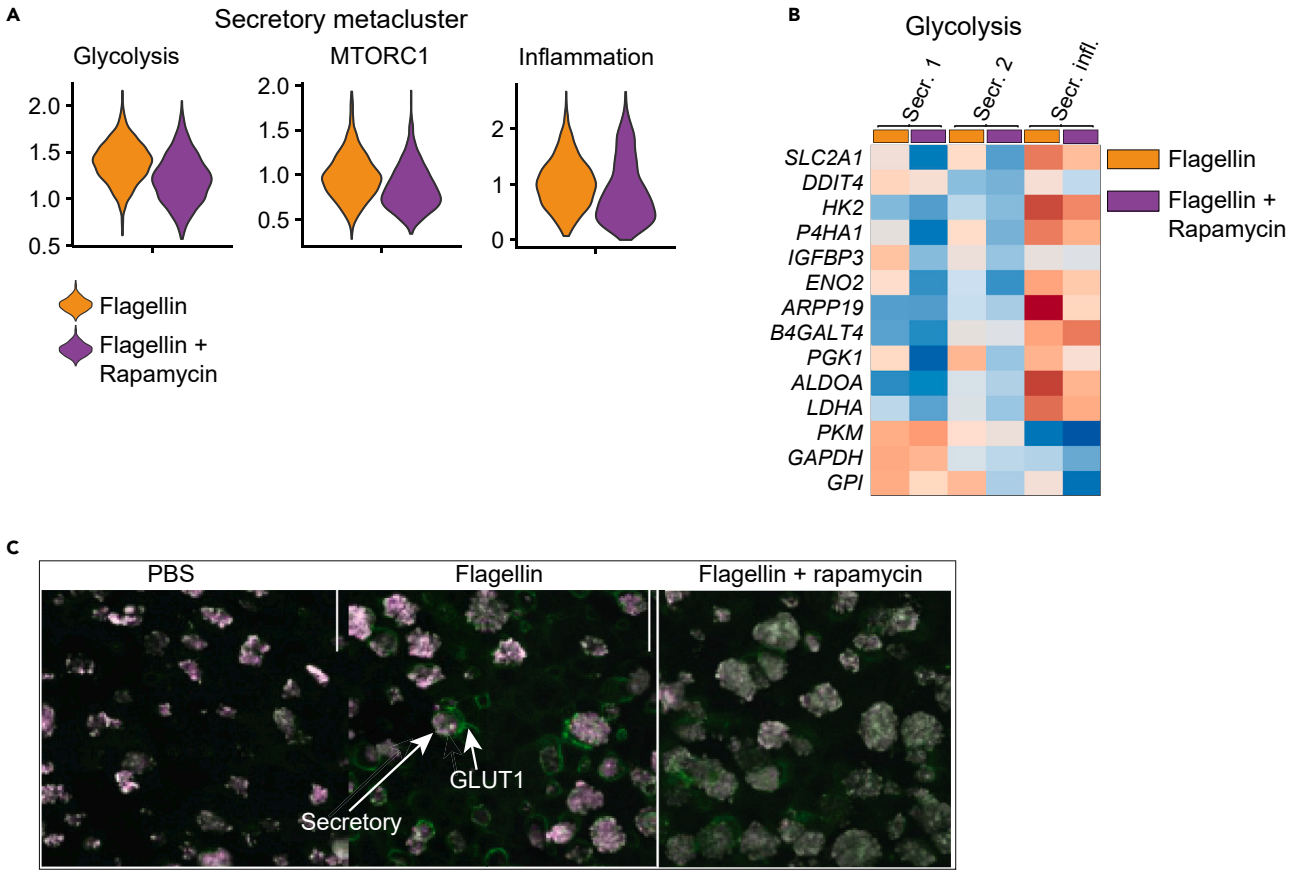

Figure 5. Rapamycin induces a transcriptional profile of reduced glycolysis and inflammation, and decreases GLUT1 expression on secretory cells

(A) Violin plots of the gene signature scores for glycolysis, mTOR and inflammation between cells in the secretory metacluster, either stimulated with flagellin or flagellin + rapamycin. Scores for other metabolic signatures are shown in Figure S4.

(B) Heatmap depicting the average scaled expression of genes related to glycolysis, split between the secretory cell clusters and the experimental condition (flagellin, or flagellin + rapamycin).

(C) Confocal microscopy showing HBE cells co-stained for GLUT1 (green) and secretory cells (purple; MUC5B^{+}) in the indicated conditions.

Incubation with rapamycin diminishes the upregulation of these transcriptomic pathways and results in a specifically decreased abundance of secretory inflammatory cells.

DISCUSSION

The respiratory epithelium plays a crucial role in innate defense against pathogens that invade the airways. We recently showed that the bacterial component flagellin activates HBE cells by increasing intracellular glycolysis through an mTOR dependent mechanism.[7] The airway wall consists of several cell types with distinct functions[2] and we here argued that our primary HBE cell cultures growing at air-liquid interface may be a suitable model to study the involvement of different cell types in the metabolic rewiring and inflammatory responses induced by flagellin. We used scRNA-seq to disclose seven cell clusters in HBE cells, of which flagellin specifically increased the abundance of inflammatory basal and inflammatory secretory cells. Remarkably, only inflammatory secretory cells displayed upregulation of genes involved in mTOR signaling and glycolysis in response to flagellin and inhibition of mTOR by rapamycin reversed this flagellin effect, as well as inflammatory gene transcription in this cell subset. Collectively, these data identify inflammatory secretory cells as the target of flagellin-induced glycolysis and inflammation in the airway epithelium.

Many studies that investigated the immune responses in respiratory epithelial cells made use of cell lines, which fail to recapitulate the cellular heterogeneity in the airway wall. This prompted us to use primary HBE cell cultures in air-liquid interface, which more resemble the cellular composition and physiological environment in the human airways, to study the metabolic regulation of mucosal immunology in the respiratory tract.[7,8] scRNA-seq analyses have added an extra layer of information about the human airways, revealing distinct cell types that previously had not been recognized by conventional methods such as microscopy.[2,20] We here leveraged this technique to study cell-specific effects of flagellin in HBE cultures and the role of the mTOR pathway herein. Clear flagellin effects were detected in the inflammatory clusters within basal and secretory metaclusters, while ionocytes and ciliated cells were

non-responsive. In accordance, the Human Protein Atlas (https://www.proteinatlas.org) reports the strongest expression of the gene encoding TLR5, the signaling receptor for flagellin, in basal and secretory cells in the human airways, with relatively low expression levels in ionocytes and ciliated cells. Our current data add to this that within the basal and secretory cell metaclusters, subclusters can be identified with distinct responsiveness to flagellin. Among these, inflammatory secretory cells responded to flagellin with an upregulation of genes regulating the glycolysis and mTOR pathways, and inhibition of the mTOR pathway by rapamycin strongly reduced the abundance of this cell subset and its inflammatory gene transcription, suggesting that our previous finding of flagellin-induced mTOR-driven glycolysis in HBE cultures is driven by inflammatory secretory cells.[7] Secretory (goblet) cells are important for key immune functions such as secretion of mucus and antimicrobial peptides.[2] As such, the current data shed light on the interaction between metabolism and mucosal immunity at single cell resolution.

Besides its effect on secretory inflammatory cells, flagellin also enhanced the expression of multiple genes in basal inflammatory cells. Some gene pathways upregulated by flagellin in basal inflammatory cells overlapped with those increased in secretory inflammatory cells, including hypoxia, the P53 pathway, apoptosis, and TNF signaling via NFkB, while others were restricted, for example, androgen response (in secretory inflammatory cells) and reactive oxygen species pathway (in basal inflammatory cells). Importantly, unlike secretory inflammatory cells, basal inflammatory cells did not show upregulated glycolysis and MTOR signaling pathways, suggesting that these cell subtypes rely on distinct metabolic pathways. Indeed, basal inflammatory cells displayed enhanced expression of genes encoding proteins implicated in oxidative phosphorylation. As compared with glycolysis, oxidative phosphorylation provides energy, in the form of ATP, in a highly efficient manner.[3–5] Myeloid cells stimulated with TLR agonists mainly generate energy through glycolysis rather than oxidative phosphorylation, similar to what we report here for secretory inflammatory cells. Future studies should determine the role of oxidative phosphorylation in flagellin-induced gene transcription in basal inflammatory cells, for example, by experiments using the inhibitor oligomycin.[5] Such additional investigations may provide a more complete understanding of the heterogeneity and functional implications of different cell subsets in the airway epithelium during inflammation.[24]

Flagellin increased the expression of androgen response genes in secretory inflammatory cells. Knowledge of cross talk between TLR signaling and androgen responses is limited. In concordance with our findings, activation of TLR4 (which triggers a signaling cascade that is highly similar to TLR5) increases androgen receptor expression and activity in ovarian cancer cells. Androgen receptors are broadly expressed in a variety of immune and non-immune cells,[25–27] and androgens[28] regulate multiple biological processes in the lung.[29] Ample evidence indicates that activation of androgen receptors in the airways mitigate type 2 allergic airway inflammation.[30,31] Indeed, mouse models have shown that androgen signaling by several immune cells contribute to inhibition of lung inflammation during experimental asthma.[32–35] In agreement, high androgen receptor expression in the bronchus were associated with better lung function and fewer symptoms in human asthma.[36] Conversely, low androgen receptor expression in the human airways was associated with elevated odds of asthma.[37] Androgen receptor signaling may also inhibit detrimental inflammatory responses during influenza A infection.[38] It remains to be established through which mechanism flagellin enhances androgen response genes in HBE cells.

scRNA-seq analyses provide extraordinary "snapshot" information about the dynamic cellular composition of the airways. Distinct cell types identified by scRNA-seq can represent cells at different differentiation stages. Pseudotime analyses, a computational method that orders cells according to their trajectory or lineage in time, have indicated that secretory cells can function as precursor for ciliated cells.[39] On the other hand, basal cells are considered multipotent stem cells from which other major subpopulations, including secretory and ciliated cells, originate.[40] Hence, our current results suggest that cells contained within the human airways can acquire or lose metabolic programs that support their inflammatory properties during their trajectories of differentiation.

Knowledge of the interaction between cellular metabolism and the capacity to mount an energy demanding inflammatory response is mainly derived from studies in lymphocytes and myeloid cells.[3–7] In these cells mTOR activation can have distinct effects, which may relate to differences in experimental conditions and the intrinsic complexity of the mTOR pathway. The present study, taken together with our previous report using bulk HBE cells,[7] points at a proinflammatory immune stimulating role of mTOR in flagellin-stimulated HBE cells. In agreement, we showed that flagellin administered via the airways of mice increased the expression of epithelial-cell specific immune mediators such as Cxcl1, Cxcl2 and Csf3 in bronchial brushes by an mTOR dependent mechanism.[7]

Flagellin is part of the bacterial flagellum, a surface filament important for bacterial motility.[9] Flagellated bacteria are sensed in the airway lumen at the apical site of the mucosa through TLR5, which initiates a brisk immune response. The potency of flagellin to elicit an innate response in the respiratory epithelium has made it an attractive candidate for an immune enhancing strategy in the airways during pneumonia.[9] The present study shows that flagellin specifically targets cellular subsets within the human airways, and that flagellin-induced proinflammatory effects in inflammatory secretory cells are regulated by the mTOR pathway. These findings advance our understanding of the regulation of mucosal immunology during infections with flagellated bacteria and provide novel information on how flagellin modulates immune functions in the airways.

Limitations of the study

This study made use of scRNA-seq to obtain insight into the responsiveness of distinct cell types in human airways to flagellin; results need to be confirmed at protein and metabolite level. Furthermore, our measurements provide a "snapshot" indication of dynamic metabolic changes; while technically challenging it would be of great interest to determine metabolic fluxes using labeled metabolites such as glucose at single cell level. While HBE cultures reflect the heterogeneity of the human airways, other cell types present in the bronchoalveolar space such as macrophages, monocytes, and lymphocytes may impact the responsiveness of cell subsets in the airways.

STAR★METHODS

Detailed methods are provided in the online version of this paper and include the following:

- KEY RESOURCES TABLE
- RESOURCE AVAILABILITY
  - Lead contact
  - Materials availability
  - Data and code availability
- EXPERIMENTAL MODEL AND STUDY PARTICIPANT DETAILS
- METHOD DETAILS
  - HBE cells and stimulation
  - Intracellular chemokine staining for flow cytometry analysis
  - Single-cell library generation and sequencing
  - Data analysis
  - Confocal microscopy
- QUANTIFICATION AND STATISTICAL ANALYSIS

SUPPLEMENTAL INFORMATION

Supplemental information can be found online at https://doi.org/10.1016/j.isci.2024.110662.

ACKNOWLEDGMENTS

Ivan Ramirez-Moral was funded by the Era-Net JPIAMR/ZonMW (grant 50-52900-98-201). Part of this work was funded by European Union H2020 (FAIR project, grant 847786). The authors thank Marja E. Jakobs (Core Facility Genomics, Amsterdam-UMC) for her technical support during the single cell RNA sequencing pipeline and Daisy Picavet and Ron Hoebe (Cellular Imaging Core Facility, Amsterdam-UMC) for helping in the acquisition and analysis of confocal microscopy images.

AUTHOR CONTRIBUTIONS

Conceptualization: I.R.-M. and T.v.d.P. Methodology: I.R.-M., K.d.H., S.v.L., X.Y., and F.A.V.B. Validation: I.R.-M., A.R.S., J.M.B., and F.A.V.B. Formal analysis: I.R.-M., A.R.S., J.M.B., and F.A.V.B. Investigation: I.R.-M., and F.A.V.B. Resources: T.v.d.P. and M.D.d.J. Writing - Original draft: I.R-M. A.R.S. and T.v.d.P. Writing - review and editing: I.R.-M., A.R.S., J.M.B., F.A.V.B., A.F.d.V., K.d.H., S.v.L., X.Y., M.D.d.J., and T.v.d.P. Visualization: I.R.-M., A.R.S., J.M.B., and F.A.V.B. Funding acquisition: T.v.d.P. All authors have read and reviewed the manuscript.

DECLARATION OF INTERESTS

The authors declare no competing interests.

Received: April 22, 2023
Revised: December 30, 2023
Accepted: July 31, 2024
Published: August 3, 2024

REFERENCES

1. Iwasaki, A., Foxman, E.F., and Molony, R.D. (2016). Early local immune defences in the respiratory tract. Nat. Rev. Immunol. *17*, 7–20. https://doi.org/10.1038/nri.2016.117.
2. Hewitt, R.J., and Lloyd, C.M. (2021). Regulation of immune responses by the airway epithelial cell landscape. Nat. Rev. Immunol. *21*, 347–362. https://doi.org/10.1038/S41577-020-00477-9.
3. O'Neill, L.A.J., Kishton, R.J., and Rathmell, J. (2016). A Guide to Immunometabolism for Immunologists. Nat. Rev. Immunol. *16*, 553–565. https://doi.org/10.1038/nri.2016.70.
4. Norata, G.D., Caligiuri, G., Chavakis, T., Matarese, G., Netea, M.G., Nicoletti, A., O'Neill, L., and Marelli-Berg, F.M. (2015). The Cellular and Molecular Basis of Translational Immunometabolism. Immunity *43*, 421–434. https://doi.org/10.1016/j.immuni.2015.08.023.
5. Stienstra, R., Netea-Maier, R.T., Riksen, N.P., Joosten, L.A.B., and Netea, M.G. (2017). Specific and Complex Reprogramming of Cellular Metabolism in Myeloid Cells during Innate Immune Responses. Cell Metabol. *26*, 142–156. https://doi.org/10.1016/j.cmet.2017.06.001.
6. Jung, J., Zeng, H., and Horng, T. (2019). Metabolism as a guiding force for immunity. Nat. Cell Biol. *21*, 85–93. https://doi.org/10.1038/s41556-018-0217-x.
7. Ramirez-Moral, I., Yu, X., Butler, J.M., van Weeghel, M., Otto, N.A., Ferreira, B.L., Maele, L.V., Sirard, J.C., de Vos, A.F., de Jong, M.D., et al. (2021). mTOR-driven glycolysis governs induction of innate immune responses by bronchial epithelial cells exposed to the bacterial component flagellin. Mucosal Immunol. *14*, 594–604. https://doi.org/10.1038/S41385-021-00377-8.
8. Ramirez-Moral, I., Ferreira, B.L., Butler, J.M., van Weeghel, M., Otto, N.A., de Vos, A.F., Yu, X., de Jong, M.D., Houtkooper, R.H., and van der Poll, T. (2022). HIF-1α Stabilization in Flagellin-Stimulated Human Bronchial Cells Impairs Barrier Function. Cells *11*, 391. https://doi.org/10.3390/cells11030391.
9. Vijayan, A., Rumbo, M., Carnoy, C., and Sirard, J.C. (2018). Compartmentalized Antimicrobial Defenses in Response to Flagellin. Trends Microbiol. *26*, 423–435. https://doi.org/10.1016/j.tim.2017.10.008.
10. Lamkanfi, M., and Dixit, V.M. (2012). Inflammasomes and their roles in health and disease. Annu. Rev. Cell Dev. Biol. *28*,

137–161. https://doi.org/10.1146/annurev-cellbio-101011-155745.

11. Hajam, I.A., Dar, P.A., Shahnawaz, I., Jaume, J.C., and Lee, J.H. (2017). Bacterial flagellin-a potent immunomodulatory agent. Exp. Mol. Med. *373*, e373. https://doi.org/10.1038/emm.2017.172.
12. Muñoz, N., Van Maele, L., Marqués, J.M., Rial, A., Sirard, J.C., and Chabalgoity, J.A. (2010). Mucosal administration of flagellin protects mice from Streptococcus pneumoniae lung infection. Infect. Immun. *78*, 4226–4233. https://doi.org/10.1128/IAI.00224-10.
13. Porte, R., Fougeron, D., Muñoz-Wolf, N., Tabareau, J., Georgel, A.F., Wallet, F., Paget, C., Trottein, F., Chabalgoity, J.A., Carnoy, C., and Sirard, J.C. (2015). A Toll-Like Receptor 5 Agonist Improves the Efficacy of Antibiotics in Treatment of Primary and Influenza Virus-Associated Pneumococcal Mouse Infections. Antimicrob. Agents Chemother. *59*, 6064–6072. https://doi.org/10.1128/AAC.01210-15.
14. Matarazzo, L., Casilag, F., Porte, R., Wallet, F., Cayet, D., Faveeuw, C., Carnoy, C., and Sirard, J.C. (2019). Therapeutic synergy between antibiotics and pulmonary Toll-like receptor 5 stimulation in antibiotic-sensitive or -resistant pneumonia. Front. Immunol. *10*, 440134. https://doi.org/10.3389/FIMMU.2019.00723.
15. Lopez-Galvez, R., Fleurot, I., Chamero, P., Trapp, S., Olivier, M., Chevaleyre, C., Barc, C., Riou, M., Rossignol, C., Guillon, A., et al. (2021). Airway administration of flagellin regulates the inflammatory response to pseudomonas aeruginosa. Am. J. Respir. Cell Mol. Biol. *65*, 378–389. https://doi.org/10.1165/RCMB.2021-0125OC.
16. Pérez-Cruz, M., Koné, B., Porte, R., Carnoy, C., Tabareau, J., Gosset, P., Trottein, F., Sirard, J.C., Pichavant, M., and Gosset, P. (2021). The Toll-Like Receptor 5 agonist flagellin prevents Non-typeable Haemophilus influenzae-induced infection in cigarette smoke-exposed mice. PLoS One *16*, e0236216. https://doi.org/10.1371/JOURNAL.PONE.0236216.
17. Davis, J.D., and Wypych, T.P. (2021). Cellular and functional heterogeneity of the airway epithelium. Mucosal Immunol. *14*, 978–990. https://doi.org/10.1038/s41385-020-00370-7.
18. Deprez, M., Zaragosi, L.E., Truchi, M., Becavin, C., Ruiz García, S., Arguel, M.J., Plaisant, M., Magnone, V., Lebrigand, K., Abelanet, S., et al. (2020). A single-cell atlas of the human healthy airways. Am. J. Respir. Crit. Care Med. *202*, 1636–1645. https://doi.org/10.1164/RCCM.201911-2199OC.
19. Garcıá, S.R., Deprez, M., Lebrigand, K., Cavard, A., Paquet, A., Arguel, M.J., Magnone, V., Truchi, M., Caballero, I., Leroy, S., et al. (2019). Novel dynamics of human mucociliary differentiation revealed by single-cell RNA sequencing of nasal epithelial cultures. Development *146*, dev177428. https://doi.org/10.1242/DEV.177428.
20. Vieira Braga, F.A., Kar, G., Berg, M., Carpaij, O.A., Polanski, K., Simon, L.M., Brouwer, S., Gomes, T., Hesse, L., Jiang, J., et al. (2019). A cellular census of human lungs identifies novel cell states in health and in asthma. Nat. Med. *25*, 1153–1163. https://doi.org/10.1038/S41591-019-0468-5.
21. Liberzon, A., Birger, C., Thorvaldsdóttir, H., Ghandi, M., Mesirov, J.P., and Tamayo, P. (2015). The Molecular Signatures Database Hallmark Gene Set Collection. Cell Syst. *1*, 417–425. https://doi.org/10.1016/J.CELS.2015.12.004.
22. Sanrattana, W., Maas, C., and de Maat, S. (2019). SERPINs-From Trap to Treatment. Front. Med. *6*, 25. https://doi.org/10.3389/fmed.2019.00025.
23. Zuo, W.-L., Rostami, M.R., Leblanc, M., Kaner, R.J., O'beirne, S.L., Mezey, J.G., Leopold, P.L., Quast, K., Visvanathan, S., Fine, J.S., et al. (2020). Dysregulation of Club Cell Biology in Idiopathic Pulmonary Fibrosis. PLoS One *15*, e0237529. https://doi.org/10.1371/journal.pone.0237529.
24. Pereverzeva, L., van Linge, C.C.A., Schuurman, A.R., Klarenbeek, A.M., Ramirez Moral, I., Otto, N.A., Peters-Sengers, H., Butler, J.M., Schomakers, B.V., van Weeghel, M., et al. (2022). Human alveolar macrophages do not rely on glucose metabolism upon activation by lipopolysaccharide. Biochim. Biophys. Acta, Mol. Basis Dis. *1868*, 166488. https://doi.org/10.1016/j.bbadis.2022.166488.
25. Huang, S.L., Chang, T.C., Chao, C.C.K., and Sun, N.K. (2020). Role of the TLR4-androgen receptor axis and genistein in taxol-resistant ovarian cancer cells. Biochem. Pharmacol. *177*, 113965. https://doi.org/10.1016/J.BCP.2020.113965.
26. Huang, S.L., Chang, T.C., Chao, C.C.K., and Sun, N.K. (2021). TLR4/IL-6/IRF1 signaling regulates androgen receptor expression: A potential therapeutic target to overcome taxol resistance in ovarian cancer. Biochem. Pharmacol. *186*, 114456. https://doi.org/10.1016/J.BCP.2021.114456.
27. Davey, R.A., and Grossmann, M. (2016). Androgen Receptor Structure, Function and Biology: From Bench to Bedside. Clin. Biochem. Rev. *37*, 3–15.
28. Mikkonen, L., Pihlajamaa, P., Sahu, B., Zhang, F.P., and Jänne, O.A. (2010). Androgen receptor and androgen-dependent gene expression in lung. Mol. Cell. Endocrinol. *317*, 14–24. https://doi.org/10.1016/J.MCE.2009.12.022.
29. Verma, M.K., Miki, Y., and Sasano, H. (2011). Sex steroid receptors in human lung diseases. J. Steroid Biochem. Mol. Biol. *127*, 216–222. https://doi.org/10.1016/J.JSBMB.2011.07.013.
30. Keith, S.A. (2023). Steroid hormone regulation of innate immunity in Drosophila melanogaster. PLoS Genet. *19*, e1010782. https://doi.org/10.1371/JOURNAL.PGEN.1010782.
31. Cusack, R.P., Nagashima, A., and Sehmi, R. (2021). Airway Androgen Receptor Expression: Regulator of Sex Differences in Asthma? Am. J. Respir. Crit. Care Med. *204*, 243–245. https://doi.org/10.1164/RCCM.202104-0869ED.
32. Ejima, A., Abe, S., Shimba, A., Sato, S., Uehata, T., Tani-Ichi, S., Munakata, S., Cui, G., Takeuchi, O., Hirai, T., et al. (2022). Androgens Alleviate Allergic Airway Inflammation by Suppressing Cytokine Production in Th2 Cells. J. Immunol. *209*, 1083–1094. https://doi.org/10.4049/JIMMUNOL.2200294.
33. Fuseini, H., Yung, J.A., Cephus, J.Y., Zhang, J., Goleniewska, K., Polosukhin, V.V., Peebles, R.S., and Newcomb, D.C. (2018). Testosterone Decreases House Dust Mite–Induced Type 2 and IL-17A–Mediated Airway Inflammation. J. Immunol. *201*, 1843–1854. https://doi.org/10.4049/JIMMUNOL.1800293.
34. Laffont, S., Blanquart, E., Savignac, M., Cénac, C., Laverny, G., Metzger, D., Girard, J.P., Belz, G.T., Pelletier, L., Seillet, C., and Guéry, J.C. (2017). Androgen signaling negatively controls group 2 innate lymphoid cells. J. Exp. Med. *214*, 1581–1592. https://doi.org/10.1084/JEM.20161807.
35. Becerra-Díaz, M., Strickland, A.B., Keselman, A., and Heller, N.M. (2018). Androgen and androgen receptor as enhancers of M2 macrophage polarization in allergic lung inflammation. J. Immunol. *201*, 2923–2933. https://doi.org/10.4049/JIMMUNOL.1800352.
36. Zein, J.G., McManus, J.M., Sharifi, N., Erzurum, S.C., Marozkina, N., Lahm, T., Giddings, O., Davis, M.D., DeBoer, M.D., Comhair, S.A., et al. (2021). Benefits of airway androgen receptor expression in human asthma. Am. J. Respir. Crit. Care Med. *204*, 285–293. https://doi.org/10.1164/RCCM.202009-3720OC.
37. McManus, J.M., Gaston, B., Zein, J., and Sharifi, N. (2022). Association Between Asthma and Reduced Androgen Receptor Expression in Airways. J. Endocr. Soc. *6*, bvac047. https://doi.org/10.1210/JENDSO/BVAC047.
38. Vom Steeg, L.G., Dhakal, S., Woldetsadik, Y.A., Park, H.S., Mulka, K.R., Reilly, E.C., Topham, D.J., and Klein, S.L. (2020). Androgen receptor signaling in the lungs mitigates inflammation and improves the outcome of influenza in mice. PLoS Pathog. *16*, e1008506. https://doi.org/10.1371/JOURNAL.PPAT.1008506.
39. Garcıá, S.R., Deprez, M., Lebrigand, K., Cavard, A., Paquet, A., Arguel, M.J., Magnone, V., Truchi, M., Caballero, I., Leroy, S., et al. (2019). Novel dynamics of human mucociliary differentiation revealed by single-cell RNA sequencing of nasal epithelial cultures. Development *146*, dev177428. https://doi.org/10.1242/dev.177428.
40. Rock, J.R., Onaitis, M.W., Rawlins, E.L., Lu, Y., Clark, C.P., Xue, Y., Randell, S.H., and Hogan, B.L.M. (2009). Basal cells as stem cells of the mouse trachea and human airway epithelium. Proc. Natl. Acad. Sci. USA *106*, 12771–12775. https://doi.org/10.1073/PNAS.0906850106.
41. Fulcher, M.L., and Randell, S.H. (2013). Human nasal and tracheo-bronchial respiratory epithelial cell culture. Methods Mol. Biol. *945*, 109–121. https://doi.org/10.1007/978-1-62703-125-7_8.
42. Stuart, T., Butler, A., Hoffman, P., Hafemeister, C., Papalexi, E., Mauck, W.M., Hao, Y., Stoeckius, M., Smibert, P., and Satija, R. (2019). Comprehensive Integration of Single-Cell Data. Cell *177*, 1888–1902.e21.

STAR★METHODS

KEY RESOURCES TABLE

REAGENT or RESOURCE	SOURCE	IDENTIFIER
Antibodies		
anti-p63	Abcam	AB124762
anti-p63	R&D Systems	AF1916
anti-MUC5B	Santa Cruz	sc-20119
donkey anti-rabbit AF488 conjugated	Life Technologies	A21206
anti-CXCL1 eFluor660 conjugated	Invitrogen	50-7515-42
ß-tubulin-Cy3	Sigma	C4585
Glut1-A488	Abcam	ab195359
anti-rabbit-AF488	Life Technologies	A21202
anti-rabbit-Cy5	Jackson Immuno Research Labs	711/175-152
anti-goat-AF488	Abcam	Ab150157
Fc Receptor binding inhibitor antibody	eBioscience	14-9161-73
Fixable viability Dye	Thermofisher	65-0865-14
TotalSeq c human hashtag antibodies	Biolegend	394673
Biological samples		
Primary HBE cells derived from healthy tracheobronchial tissue	Amsterdam University Medical Center (The Netherlands)	Study protocol 2015-122#A2301550
Chemicals, peptides, and recombinant proteins		
Flagellin from Pseudomonas aeruginosa	Invivogen	tlrl-pafla
Rapamycin	Cayman Chemical	13346
Brefeldin A	Invitrogen	00-4506-51
Liberate TM	Sigma Aldrich	5401119001
DNase I	Sigma Aldrich	EN0521
Critical commercial assays		
ProLongTM kit	ThermoFisher	P7481
Chromium Single Cell 5′ Library & Gel Bead Kit v1.1	10X Genomics	NA
Chromium Next GEM Single Cell V(D)J Reagent Kits v1.1 Rev E	10X Genomics	NA
Cytofix/Cytoperm kit	BD Biosciences	554714
Deposited data		
Raw and analyzed data	This paper	GEO GSE272188
Software and algorithms		
CellRanger 3.1	10X Genomics	NA
R package 'Seurat'	NA	NA
ImageJ	Schneider et al.7	https://imagej.nih.gov/ij/

RESOURCE AVAILABILITY

Lead contact

Prof. T. van der Poll. Contact information: t.vanderpoll@amsterdamumc.nl.

Materials availability

This study did not generate new unique reagents.

Data and code availability

Single-cell RNA-seq data have been deposited at GEO and are publicly available as of the date of publication. Accession numbers are listed in the key resources table.

EXPERIMENTAL MODEL AND STUDY PARTICIPANT DETAILS

HBE cells were derived from healthy tracheobronchial tissue obtained from a lobectomy in a patient with lung cancer at the Amsterdam University Medical Centers in the Netherlands, as previously reported.[7,8] The Institutional Review Board of Amsterdam UMC approved the study protocol (2015-122#A2301550) and written informed consent was obtained from the donor before sampling.

METHOD DETAILS

HBE cells and stimulation

HBE cells were isolated according to Fulcher's protocol.[41] In short, passage 2 (P2) to P4 passaged cells were differentiated in 24-well Transwell inserts (Corning, Corning, NY, USA) coated with human type IV placental collagen in submerged PneumaCult-Ex Plus media (StemCell Technologies, Vancouver, Canada). When cells reached confluency, the media was replaced by PneumaCult-ALI medium (StemCell Technologies) on the basolateral side and the apical side was exposed to the air, forming an air-liquid interface. The basolateral media were renewed every two or three days for around 30 days. For cell stimulation experiments, flagellin from *Pseudomonas aeruginosa* (1 μg/ml; Invivogen, Toulouse, France) was added to the apical compartment and left for 24 hours. For mTOR inhibition experiments, rapamycin (10 nM; Cayman Chemical, Ann Arbor, MI, USA) was added to the medium 1 hour prior to flagellin stimulation. After stimulation, HBE cells were digested for 30 min at 37°C in the presence of 5 mg/ml Liberase TM (Sigma; St. Louis, MO, USA) and 10 mg/ml DNase (Roche; Basel, Switzerland). Fixable Viability Dye kit (eBioscience; San Diego, CA, USA) was used to assess cell viability by FACS analysis (> 90% in all samples).

Intracellular chemokine staining for flow cytometry analysis

For intracellular chemokine experiments, 1 μl/ml of Brefeldin A (Invitrogen) was added to the culture medium at the basolateral site prior to stimulation with 1 μg/ml of flagellin (or PBS) addition to the apical side. After 3 hours of stimulation, HBEs in the inserts were digested for 30 min at 37°C with Liberase TM (5 mg/ml; Sigma-Aldrich). and DNase I (10 mg/ml; Sigma-Aldrich). Cell suspensions were filtered through a 70-μm nylon mesh or steel strainer. First, cell suspensions were incubated with a mix containing Fc Receptor binding inhibitor antibody (eBioscience) and fixable viability Dye (Thermofisher), subsequently, the following surface markers were used: anti-p63 (AB124762; Abcam), anti-MUC5B (sc-20119; Santa Cruz), donkey anti-rabbit AF488 conjugated (A21206; Life Technologies). Then, a Cytofix/Cytoperm kit (BD Biosciences) was used for cell permeabilization, staining and washing. The anti-CXCL1 eFluor660 conjugated (50-7515-42; Invitrogen) was used at the concentration recommended by the manufacturer. For phenotypic analysis by flow cytometry, data were acquired on an FACSCanto II instrument (BD Biosciences) and analysed with FlowJo software (TreeStar).

Single-cell library generation and sequencing

The Chromium Single Cell 5′ Library & Gel Bead Kit v1.1 (10X Genomics, Pleasanton, CA) was used to generate the libraries following the manufacturer's instructions. In short, we sorted 200,000 single cells per condition. Each sample was labelled with TotalSeq c human hashtag antibodies (Table S2). Samples were incubated for 30 minutes with 1 μl of antibody per sample. Thereafter, the antibody was washed three times with PBS 0.1% BSA. Cells were counted and 50,000 cells from each sample were pulled together. The pooled samples were loaded in the 10X chromium and loaded the cells on the 10X machine. Libraries were generated according to standard protocol (Chromium Next GEM Single Cell V(D)J Reagent Kits v1.1 Rev E; 10X Genomics). Libraries were sequenced using the Illumina HiSeq4000 (Illumina, San Diego, CA, USA). Each position from the 10X chip was loaded into 1 HiSeq 4000 lane.

Data analysis

All libraries were aligned using CellRanger 3.1 (10x Genomics). Cell deconvolution and analysis were performed using the R package 'Seurat'.[42] The cells were filtered based on number of features (nfeature_RNA), number of genes (nCount_RNA), and percentage of mitochondrial reads (percent.mt) using Seurat 'subset(object, subset=nCount_RNA>1000 and nCount_RNA<10,000 and nFeature_RNA>200 and percent.mt<20)'. We calculated cell cycle scores as follows: ('CellCycleScoring(Healthy_object_Cycle), s.features=s.genes, g2m.features=g2m.genes, set.ident=TRUE') using a list of S phase and G2M phase genes preloaded in Seurat. The cells were then scaled and normalized using the function 'SCTransform(object, vars.to.regress=c('nCount_RNA', 'percent.mt', 'S.Score', 'G2M.Score')). Principal components for each set of cells as shown in individual figures were identified using the 'RunPCA' function. Cells were then further processed for clustering and visualization using the Seurat functions 'FindNeighbors', 'FindClusters', and 'RunUMAP'. The number of principal components used as input was determined by using the 'ElbowPlot' function and identifying the number of the PCs which explain most of the data variance. Differential expression analysis was performed using the functions 'FindAllMarkers' or 'FindMarkers' and the following parameters: 'min.pct=0.25, logfc.threshold=0.25, assay='SCT''.

Confocal microscopy

Cells were fixed in 4% formaldehyde for 20 min and stored submerged in PBS at 4°C until analysis. HBE were permeabilized for 1 hour in 0.1% Triton-X followed by blocking in 1% BSA in PBS for 30 min. Samples were stained with the following primary antibodies: MUC5B (sc-20119; Santa Cruz Biotechnology; Dallas, TX, USA), p63 (AB124762; Abcam, Cambridge, UK) p63 (AF1916; R&D Systems; Minneapolis, MN, USA), ß-tubulin-Cy3 (C4585; Sigma) and Glut1-A488 (ab195359; Abcam). The following secondary antibodies were used: anti-rabbit-AF488 (A21202; LifeTechnologies; Carlsbad, CA, USA), anti-rabbit-Cy5 (711/175-152; Jackson Immuno Research Labs; West Grove, PA, USA) and anti-goat-AF488 (Ab150157; Abcam). The nuclei were stained using the ProLong™ kit (ThermoFisher Scientific; Waltham, MA, USA). Cell imaging was performed on a Leica SP8 confocal microscope (Leica; Wetzlar, Germany). Images are shown as maxi-projection on the z-stack planes.

QUANTIFICATION AND STATISTICAL ANALYSIS

All analyses were performed in R version 4.1.2. Enrichment analysis was performed by first generating contingency tables with the cell distributions per cluster. Next, chi-squares for the contingency tables were calculated and correlation plots were generated with the R package *corrplot*. Comparisons with at least more than two residuals of difference were considered biologically relevant. All gene expression analyses were corrected for multiple testing using the Benjamini-Hochberg method, with significance defined as an adjusted $p<0.05$. Pathway analysis was performed using Gene Set Enrichment Analysis based on the Molecular Signatures Database (MSigDB).[21]